Research Paper

EARTHQUAKE SPECTRA

Earthquake Spectra
1–30

DOI: 10.1177/8755293021102860 9
journals.sagepub.com/home/eqs
SAGE

Performance of externally bonded fiber-reinforced polymer retrofits in the 2018 Cook Inlet Earthquake in Anchorage, Alaska

Jovan Tatar, M.EERI[1], Siamak Sattar, M.EERI[2], David Goodwin[3], Sandra Milev[1], Shafique Ahmed[4], Jazalyn Dukes[2], and Christopher Segura, M.EERI[2]

Abstract

As part of the effort to improve the seismic performance of buildings in Alaska (AK), many of the deficient structures in Anchorage, AK, were retrofitted—some with externally bonded fiber-reinforced polymer (EBFRP) composite systems. The 2018 magnitude 7.1 Cook Inlet earthquake that impacted the same region offered an opportunity to evaluate the performance of EBFRP retrofits in a relatively high-intensity earthquake. This study summarizes the following findings of this field investigation: (1) the performance of EBFRP-retrofitted structures in the Cook Inlet earthquake and (2) the observations concerning the condition of FRP retrofits from over a decade of exposure in a subarctic environment. A deployment team from the National Institute of Standards and Technology (NIST) in collaboration with the University of Delaware (UD) Center for Composite Materials conducted post-earthquake inspections of EBFRP retrofits in multiple buildings to assess their performance during the earthquake and condition with respect to weathering. EBFRP debonding was documented with infrared thermography and acoustic sounding and the bond quality between EBFRP and concrete was assessed using pull-off tests. Visual inspections showed no major signs of earthquake damage in the EBFRP-retrofitted components. However, evaluation of debonding and pull-off test results suggested that outdoor conditions may have led to bond deterioration between EBFRP

[1]Department of Civil and Environmental Engineering, Center for Composite Materials, University of Delaware, Newark, DE, USA
[2]Earthquake Engineering Group, Engineering Laboratory, National Institute of Standards and Technology, Gaithersburg, MD, USA
[3]Infrastructure Materials Group, Engineering Laboratory, National Institute of Standards and Technology, Gaithersburg, MD, USA
[4]Echem Consultants LLC, Poughkeepsie, NY, USA

Corresponding author:
Jovan Tatar, Department of Civil and Environmental Engineering, Center for Composite Materials, University of Delaware, 301 DuPont Hall, Newark, DE 19716, USA.
Email: jtatar@udel.edu

and concrete from installation defects that grew over time, freeze–thaw expansion from moisture present at the FRP/concrete interface, differences in thermal expansion of the materials, or a combination thereof. The carbon fiber–reinforced polymer (CFRP) bond to concrete was found to be more vulnerable to outdoor exposure than the glass fiber–reinforced polymer (GFRP) bond. Earthquake effects on FRP/concrete bond could not be assessed due to the lack of baseline data.

Keywords
FRP, composites, seismic, retrofit, earthquake, Alaska, reconnaissance, field study, durability

Date received: 2 November 2020; accepted: 9 June 2021

Introduction

Since the catastrophic Great Alaskan earthquake (magnitude 9.2) struck Alaska in 1964, significant effort has been made to mitigate seismic risk in this region through building rehabilitation. Over the years, seismic design requirements evolved to provide increased seismic resiliency, and as a result, many of the deficient structures were retrofitted—some with externally bonded fiber-reinforced polymer (EBFRP) composite systems. The 2018 Cook Inlet earthquake impacted the same region that was severely damaged by the 1964 Great Alaskan earthquake and provided an opportunity to evaluate the effectiveness of EBFRP retrofits in a relatively high-intensity earthquake. Improved performance of seismically deficient reinforced concrete (RC) structures retrofitted with EBFRP has been confirmed in many studies over the last 20 years. Findings indicate that EBFRP materials are efficient in preventing brittle failure modes in concrete, weak-story failure, and large residual displacements in RC structures, providing confinement (Kobatake, 1998), higher shear resistance (Silva et al., 2007; Triantafillou, 1998), and energy dissipation (Di Ludovico et al., 2008). These findings are based on numerical models, experimental quasi-static load tests, or shake-table tests. However, data on the seismic performance of EBFRP retrofitted structures in an actual earthquake are sparse. A review of published literature on the post-earthquake reconnaissance of EBFRP-retrofitted RC structures revealed only one study that describes damage observations after the 2010 Darfield (Canterbury) earthquake (Kam et al., 2010). Based on the visual inspection of two EBFRP-retrofitted buildings, it was concluded that they performed well during the earthquake with an intensity comparable to the design earthquake. Specifically, there was no structural or non-structural damage in a three-story RC frame building where EBFRP was used to confine non-ductile columns. At the other building (two-story RC frame building with EBFRP jackets used to confine columns), flexural cracks were observed in the plastic hinge region within the FRP. It was possible to easily detect cracking by visual inspection since uncoated glass fiber–reinforced polymer (GFRP) was installed on these columns. The field study presented in this article will, for the first time, provide information on the performance of EBFRP-retrofitted structures in the United States based on post-earthquake inspection of six retrofitted structures in Anchorage, AK.

The most commonly used approaches for seismic retrofitting of RC structures with EBFRP materials include column confinement, flexural and shear strengthening of beams and walls, and strengthening of beam–column joints. Wrapping concrete columns with EBFRP provides confinement to plastic hinges, improves capacity of inadequate lap splices, and prevents buckling of the longitudinal reinforcement, which, in turn, can

improve ductility and strength of columns (Bousias et al., 2007; del Rey Castillo et al., 2018; Ma et al., 2017; Pendhari et al., 2008). Adhering EBFRP in expected plastic hinge regions improves the flexural capacity of RC beams and columns, whereas placing vertical EBFRP at wall boundary elements increases in-plane flexural strength of walls (Woods et al. 2020). Shear strengthening of walls is commonly achieved by applying horizontal EBFRP along the height of the wall. EBFRP reinforcement wrapped around beam–column joints has been shown to improve their shear capacity and ductility (Pantelides et al., 2008).

The effectiveness of EBFRP retrofits in flexural and shear strengthening of beams and walls depends on the adhesive bond strength between EBFRP and concrete. Therefore, these applications are referred to as bond-critical. However, applications such as column confinement require mere physical contact between the EBFRP and the concrete and are, thus referred to as contact-critical. Before inspecting any EBFRP RC member, it is important to know if a specific EBFRP retrofit is bond-critical or contact-critical to be able to evaluate its performance. Many examples of both types of applications were observed and documented during the post-earthquake inspection of structures in Anchorage, AK and are discussed herein.

During their service life, RC structures are often exposed to harsh environmental conditions. Effects of moisture, temperature, and freeze–thaw cycles on the performance of EBFRP-retrofitted concrete structures have been investigated, with particular focus on the bond degradation between the EBFRP and concrete. A study conducted by Al-Mahmoud et al. (2014) suggests that 300 freeze–thaw cycles in a humid environment can result in a 26% decrease in shear strength of three-point bending specimens. The extent of deterioration is highly dependent on the moisture content at the interface. Specifically, stress generated due to volumetric expansion when ice is formed at subzero temperatures is considered the main contributor to bond degradation. Results from a study conducted by Pan et al. (2018) show that concrete mechanical properties can be significantly more affected by freeze–thaw cycling than the adhesive or the EBFRP, although concrete fairs better under freeze–thaw conditions when adequately air entrained (Green et al., 2006).

Based on bond strength data from various literature sources, Pan et al. (2018) proposed an interfacial fracture energy degradation model of the EBFRP/concrete bond that was used to predict the service lives of externally bonded carbon fiber–reinforced polymer (CFRP) and GFRP as a function of the number of freeze–thaw cycles. They predicted usable service life of 12 and 51 years for CFRP and GFRP, respectively, which indicates significant differences in durability between CFRP and GFRP due to freeze–thaw. Reasons for differences in deterioration of the bond to concrete for CFRP compared to GFRP during freeze/thaw were not explained by Pan et al. Green et al. (2000) point out that incompatibility in coefficients of thermal expansion (CTEs) between EBFRP and concrete may be the underlying degradation mechanism during freeze–thaw cycling. However, there is limited information on whether CTE is a factor contributing to more severe CFRP bond deterioration relative to GFRP bond deterioration. In a study conducted by Sheikh and Tam (2007) that also investigated effect of freeze/thaw cycles on EBFRP/concrete bond strength, differences between CFRP and GFRP were not as significant as Pan et al. suggested. Based on results presented in the study by Sheikh and Tam (2007), an environmental reduction factor of 0.65 in ACI 440.2R (American Concrete Institute (ACI)) largely underestimates GFRP/concrete bond strength. ACI 440.2R (2017) accounts for the effect of fiber type on the long-term behavior of a composite strengthening system only through the reduction in strength of the EBFRP composite alone according to service

environment. However, EBFRP–concrete bond strength is more likely to be affected by deterioration than the composite itself (Blackburn et al., 2015; Tatar et al., 2018a, 2018b, 2019), which is why a different design approach was proposed by Tatar and Hamilton (2016c) that explicitly takes into account the durability of bond.

Accelerated conditioning in a laboratory setting can provide valuable insight into the long-term durability of composites, but more field data are necessary to validate accelerated conditioning protocols, especially those used for strength reduction factors (Goodwin et al., 2019; Tatar and Hamilton, 2016a). So far, only a limited number of field studies investigated aging of EBFRP under realistic conditions Tatar and Milev (2021). A report by Hamilton et al. (2017) presents results from EBFRP bond strength evaluation conducted on bridges exposed to a marine environment in Florida for up to 15 years. EBFRP repairs were found to have a satisfactory structural performance as the majority of bond pull-off tests exceeded the minimum bond strength requirement of 1.4 MPa (200 lbf/in^2) (ACI 440.2R). However, a significant number of adhesive failure modes were observed indicating that some bond degradation may have occurred. Considerably lower bond strength (0.1 MPa to 1.5 MPa (15 to 220 lbf/in^2)) and mostly adhesive failure modes were recorded by Al Azzawi et al. (2018) on bridge piles, also located in Florida. Differences in EBFRP performance observed by Hamilton et al. (2017) and Al Azzawi et al. (2018) in the marine environment, indicate that bond durability is sensitive to the installation process, surface preparation, type of resin, ambient conditions during installation, and specific location of strengthened member (e.g., piles are exposed to water immersion during tidal fluctuations unlike bridge girders). Pallempati et al. (2016) reported that 58% of pull-off tests conducted on bridges in Texas exhibited a cohesive failure mode, and most of them (79%) exceeded the required minimum strength of 1.4 MPa. Correlation between the age of repairs (between 2 and 8 years) and the percentage of cohesive failures could not be established. To connect laboratory data with field data, Myers and Sawant (2008) presented a strength degradation model for EBFRP-repaired bridges, validated against field data. Using an analytical model that incorporates bond strength reduction factor and steel loss factor, authors predict a 17-year service life for a CFRP-strengthened bridge in Missouri.

Field data from cold regions are sparse. Siavashi et al. (2019) evaluated fully wrapped, EBFRP-strengthened columns of a bridge in Michigan after 15 years of exposure and reported 20% lower bond strength on the column side facing approaching vehicles. Based on the degradation model, the authors proposed an environmental reduction factor for the bond between 0.48 and 0.56 after 50 years of service. A slightly greater reduction factor of 0.60 for the bond was also proposed by Tatar and Hamilton (2016b, 2016c), mostly based on test results of beams exposed to water immersion/moisture at different temperatures. Field evaluation of four EBFRP-strengthened bridges in Canada, exposed to a relatively cold climate for up to 13 years (Banthia et al., 2010) showed a large variation in the measured mean bond strength (0.83 MPa to 3.54 MPa (120 to 513 lbf/in^2)). Atadero and Allen (2013), who evaluated the performance of EBFRP after 8 years of service on a concrete bridge in Colorado, reported that debonding occurred at various locations; bond pull-off strengths also experienced an average 35% reduction. Based on observations of a CFRP-repaired bridge in Salt Lake City, Reay and Pantelides (2006) concluded that CFRP reinforcement was effective after 3 years of service, but indicated that environmental conditions (freeze–thaw cycles and de-icing salts) decreased the bond strength between CFRP and concrete. Hag-Elsafi et al. (2004) evaluated a 2-year-old CFRP repair on a concrete bridge in Rensselaer County, New York and found that CFRP–concrete bond quality did not change based on load test and infrared (IR) thermography data. Limited

field data from the open United States and Canadian literature indicate that further investigation of the environmental durability of EBFRP is necessary, especially for EBFRP in use on structures. A deployment team from the National Institute of Standards and Technology (NIST) in collaboration with the University of Delaware (UD) Center for Composite Materials (hereafter referred to as the reconnaissance team), conducted the post-earthquake inspections of multiple structures with EBFRP retrofits in January 2019 and September 2019 visits to Anchorage, AK. A comparison between the conditions of interior and exterior EBFRP retrofits were also made to describe the impact of environmental factors on EBFRP–concrete bond durability with potential implications on EBFRP retrofit performance in future earthquakes. Observations from this study, which highlight the challenges of post-earthquake inspection of EBFRP-retrofitted buildings will be valuable for future development of techniques and guidelines for field inspection.

Earthquake characteristics

On 30 November 2018, at 9:29 a.m. local time, a magnitude (M_w) 7.1 earthquake struck north of Anchorage, Alaska, United States. The epicenter of the earthquake was about 16 km north of Anchorage in a less populated area. This earthquake occurred as a result of normal faulting at a depth of 47 km. Multiple aftershocks occurred after this earthquake; the largest aftershock was a 5.7 M_w earthquake on 30 November. The recorded peak ground acceleration in the most populated areas of the region, that is, Anchorage and Eagle River, ranged from 0.04 to 0.55 g. Figure 1 shows the response spectra for the east–west component of the recorded ground motions at three different sites in Anchorage. This figure shows that for structural periods greater than 0.3 s, all three response spectra are less than the design-level earthquake.

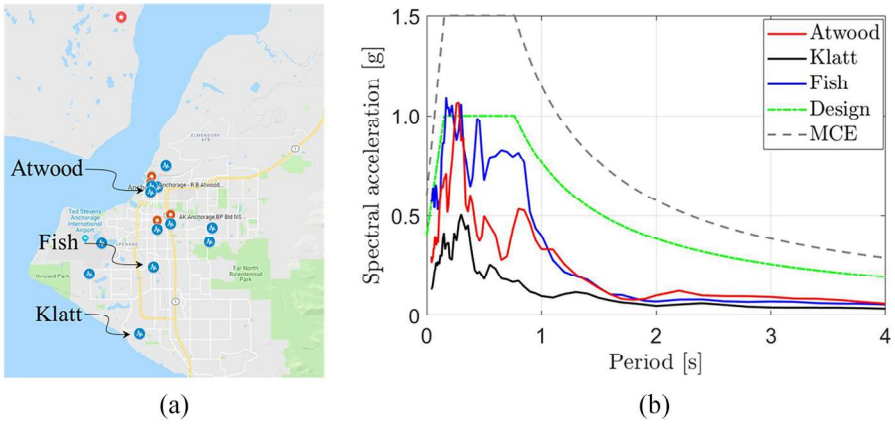

Figure 1. (a) Location of Atwood, Fish, and Klatt stations in Anchorage, AK, (b) response spectra of the E–W component of the recorded ground motions in the 2018 Anchorage earthquake (site class D is assumed).

Inspected structures

The reconnaissance team inspected seven RC structures with externally bonded EBFRP reinforcement in Anchorage, AK. Most of the EBFRP were employed as seismic retrofit systems, and others were in use for gravity strengthening and repair. Table 1 summarizes the characteristics of the inspected structures. The list in Table 1 only encompasses the EBFRP retrofits seen during inspections and may not cover all EBFRP retrofit types in a given structure. The last column in Table 1 summarizes the inspection methods used in the field; the first four structures were inspected visually. More in-depth inspections were performed at the McKinley Tower (MKT) and the Ted Stevens International Airport (TSIA).

Scope of inspections

Inspections consisted of visual inspections, acoustic sounding, IR thermography, and bond pull-off tests. Each technique is briefly described in the following sections.

Visual inspection

Visual inspection is the first tier of inspection that can provide critical information on the state of the structure or component. In this reconnaissance effort, all inspections involved photographic evidence collection and conversations with building managers or building owners. When possible, historical information on the EBFRP material installation, manufacturer, retrofit purpose, and inspection practices were obtained. FRP retrofit access varied significantly at different sites and within sites. During inspections, the team faced accessibility problems as many EBFRP retrofits were located behind drywall, panels, or other architectural finishes. This is a challenge that may require further-improved access considerations (e.g., access panels) or assessment tools and techniques for new and existing EBFRP retrofits to assess their performance after future earthquakes.

Acoustic sounding and qualitative IR thermography

Acoustic sounding and IR thermography can be considered the second tier of inspection. These techniques can be used to locate debonded areas of the EBFRP retrofits. Identification of debonded areas is critical as it may be an indication of degradation, poor installation, or failure of the bond between EBFRP and concrete substrate, which in turn can lead to poor performance of the retrofitted component. Acoustic sounding was conducted by light tapping of the EBFRP surface with a small steel hammer and listening to the audible response of the EBFRP to detect debonding. The debonded areas identified by acoustic sounding were marked with pieces of blue painter's tape and photographed.

A few columns were inspected for debonding using qualitative IR thermography (Brown, 2005), a more sophisticated technique. This involved heating the surface of the EBFRP with two 500 W halogen lamps for a few minutes at the same approximate distance ($\approx$ 20 cm), followed by measuring the surface temperature with a FLIR F8 portable IR camera. Although this technique was more thorough at detecting debonded areas relative to acoustic sounding, it was a time-consuming process; for example, it took more than

Table 1. Summary information of the inspected buildings.

Structure name	Year constructed	Year retrofitted	Retrofit material	Retrofit location	Inspection methods
Anchorage Water and Wastewater Treatment Plant—Heat Exchange Facility	1988	2015	CFRP	Indoor and outdoor	Visual inspection
Anchorage Water and Wastewater Treatment Plant—Water Treatment Building	1962/expanded in 1986	2018/2019	CFRP and GFRP	Indoor and water treatment facility	Visual inspection
Boney Courthouse	1973	2009	CFRP	Indoor	Visual inspection
Joint Base Elmendorf–Richardson Engineering Squadron building	1952	2012	CFRP	Indoor and outdoor	Visual inspection
Ted Stevens International Airport—South terminal (TSIA)	1968 and later	2008	CFRP	Indoor and outdoor	Visual inspection, acoustic sounding, infrared thermography, and bond pull-off tests
McKinley Tower (MKT)	1951–1952	2004	GFRP and CFRP	Indoor and outdoor	Visual inspection, acoustic sounding, and bond pull-off tests

Figure 2. Example infrared thermography and acoustic sounding results on a section of the column: (a) IR image overlapped with photography from FLIR camera (dimensions in cm), (b) photograph of the same area with FLIR camera, and (c) debonded areas marked with blue painter's tape after acoustic sounding. This figure shows a good visual match between the IR thermography and acoustic sounding results.

2 h to image one face of a column. Due to its time-consuming nature, IR thermography was only attempted on two columns (one interior and one exterior) at TSIA.

In IR thermography, hot spots typically show up in debonded areas due to slower heat dissipation by air than by the composite or concrete (Figure 2). Each of those areas was subsequently evaluated via acoustic sounding to confirm whether or not the IR signal was a "false positive." Areas that were confirmed to have air pockets by acoustic sounding were marked with a blue painter's tape. The IR signal was then used to compute the approximate area of the debonded regions. Comparing IR thermography images with the photographs that documented debonded locations indicates that qualitative IR thermography can result in many false positive readings. This is likely due to the uneven thickness of the adhesive layer, uneven thickness of the EBFRP composite, and variations in thermal properties of the concrete substrate.

Bond pull-off tests

The bond pull-off test is the third tier of inspection used to assess the tensile bond strength between an EBFRP composite retrofit and a concrete substrate (ASTM D7522, 2015). The bond pull-off test was utilized in this field study since it is commonly used as a post-installation quality control measure by EBFRP installers and inspectors according to ACI 440.2R. The pull-off tests were conducted in areas with no indication of debonding, as determined with acoustic sounding. To conduct a pull-off test, the test location was prepared by sanding to remove any paint or coating on EBFRP, followed by cleaning with acetone to eliminate surface contamination. A 5 cm steel puck was then adhered to the prepared test area using JB-Weld ClearWeld quick-set 30.3 MPa (4400 lbf/in^2 strength) epoxy adhesive. When temperatures were below freezing, the epoxy curing process was accelerated using a halogen lamp as an external heat source. Each puck was cured for at least 2 h prior to the bond pull-off test. Three pull-off tests were performed on each structural component at TSIA and MKT to assess EBFRP–concrete bond quality by measuring bond strength and assessing the failure mode. For comparison, pull-off tests were conducted on retrofitted components located inside and outside at each structure. It should be noted that longer heating times were used to adhere pucks in outdoor pull-off tests as the ambient temperature was in the −18°C to 8°C range during the January 2019 visit. During the September 2019 site visits, the outdoor temperatures ranged from −2°C to 14°C but pull-off tests were always conducted above the freezing temperature.

A diamond-tipped core saw attached to a portable drill was used to drill around the applied puck and through the EBFRP composite. Drilling proceeded until the drill-bit reached the concrete substrate. After drilling, an adhesion tester (DeFelsko PosiTest ATA) was clamped to the puck and the puck was loaded at approximately 2 kN/min loading rate until bond failure was reached. To minimize the effects of EBFRP coring on the seismic performance of EBFRP confinement, bond pull-off tests were conducted away from plastic hinge regions and column corners. The failure mode was recorded according to ASTM D7522 (2015) (Figures 3 and 4). Observed failure modes included Mode A, Mode C, Mode E, Mode F, and Mode G. Following testing, each test location was patch-repaired by a licensed contractor according to ACI 440.2R recommendations and the manufacturer's specifications.

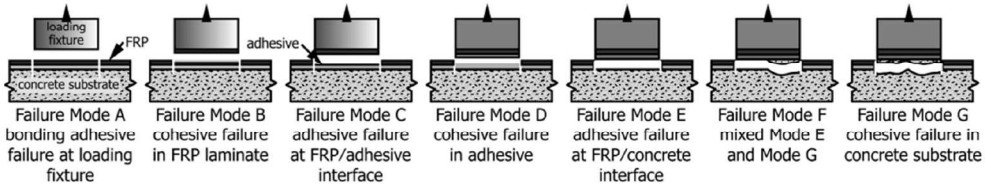

Figure 3. Pull-off test failure modes (reprinted from ASTM D7522 (2015).)

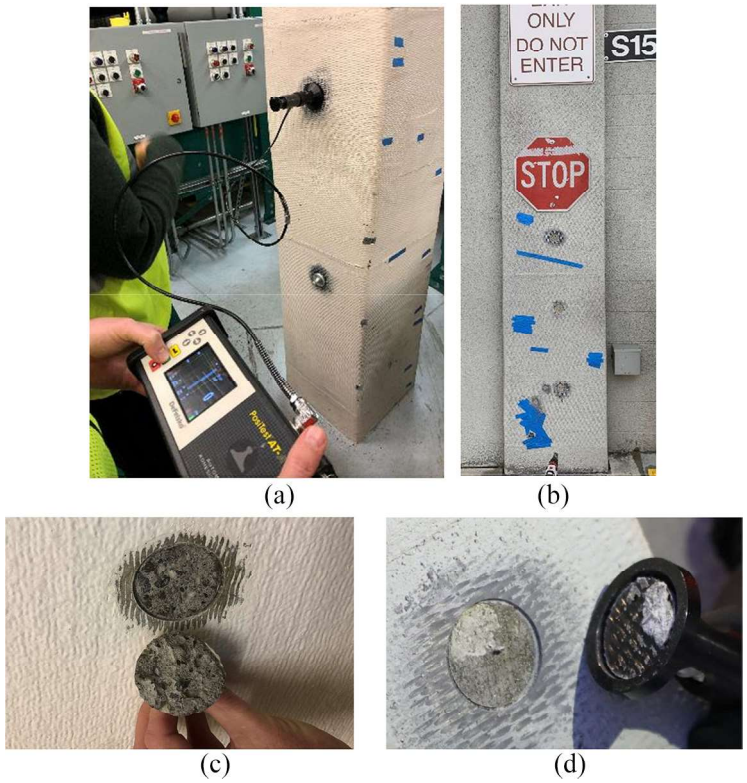

Figure 4. (a) An example of the bond pull-off test setup, (b) a column after bond-pull-off tests and typical bond pull-off test failure modes such as (c) Mode G, cohesive failure mode in concrete and (d) Mode E, interfacial adhesive failure mode.

Classification of failure modes from pull-off tests in aged field samples requires some discretion and engineering judgment due to the uncertainties associated with the application of EBFRP in the field. Some sources of variability include uneven application of paste epoxy tack coat or putty (which can be mistaken for concrete/mortar) during EBFRP installation, non-uniform surface preparation or complete lack thereof, entrapped air bubbles along the EBFRP–concrete bond line, substrate composition (e.g. concrete vs repair mortar), and variations in surface wetting with the epoxy adhesive. As Mode G is a desired failure mode indicating sound adhesion between EBFRP and substrate, one expects this failure mode to manifest itself with the following: (1) a large amount of sand and/or aggregate particles on the fractured surface and (2) a thickness of the pulled-off material that exceeds the thickness of the composite and adhesive layer by a few millimeters, at a minimum. To avoid undue confusion, any bond failure mode that did not satisfy the described two criteria was classified as an interfacial adhesive failure mode (Mode E).

Results and discussion

Anchorage water and wastewater treatment plant

Two facilities in the Anchorage water and wastewater treatment plant that were retrofitted with EBFRP were investigated in the reconnaissance effort: (1) the heat exchange facility and (2) the water treatment building. In the heat exchange facility, an EBFRP retrofit was applied to a load-bearing wall that was modified to include an opening for egress into a new extension of the original structure. As shown in Figure 5, the CFRP was applied around the perimeter of the portal to act as additional shear reinforcement. On the exterior of the building, CFRP retrofits were used to tie precast concrete panels to the frame and foundation ensuring composite behavior of the structure in a seismic event. Design plans show only the location of the EBFRP and details related to EBFRP (number of plies, dimensions and so on), but do not show details of the precast joint. Typically, precast panels are connected to the frame using steel rods and plates. However, the reconnaissance team was not able to confirm this through visual inspection of the joint. Minor cracks were noted along the column–panel joints on the interior of the building (Figure 6), but it is not clear if these cracks developed during the earthquake or were present before the earthquake. Since CFRP retrofits were covered by nonstructural elements on the building exterior, potential damage to the EBFRP that was on the opposite side of the wall shown in Figure 6 could not be assessed.

Figure 5. CFRP applied around the perimeter of the portal as denoted by red dotted lines.

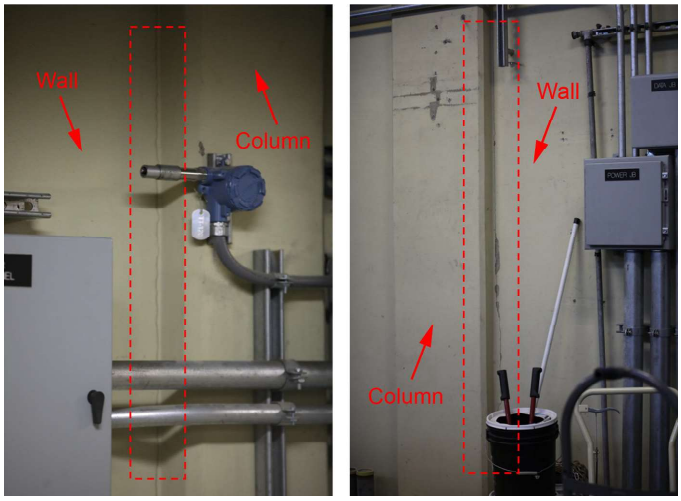

Figure 6. Cracking along column–wall joints induced by earthquake shaking. Cracks are denoted by blue dotted lines.

In the water treatment facility, CFRP was applied to increase the shear strength of joists in several rooms. Some hairline cracks were observed in the roof slab supported by the joists (Figure 7c), but it is not known whether those cracks existed before the earthquake. According to the building owner, some cracks observed in the joists (Figure 7d) existed prior to the earthquake. These cracks were likely caused by restrained shrinkage and/or temperature gradients. In addition, no damage to the CFRP or cracks traversing from uncovered concrete to areas with CFRP were observed. In addition, acoustic sounding of multiple joists revealed no defects.

In the areas with the large water storage tanks used for various treatment processes, columns, shear walls, and shear wall boundary elements were retrofitted with CFRP and GFRP. All EBFRP retrofits were covered with a gray cement-based coating to achieve a concrete-like surface finish. Boundary elements of multiple shear walls were retrofitted for flexural strengthening with CFRP and with fiber splay anchors being utilized to develop the full-design capacity of the CFRP (Figure 8). The entire area of one shear wall was wrapped with horizontally placed GFRP where the GFRP extended around the back of the wall at a length of 30 cm for confinement of the wall. All EBFRP retrofits were visually intact and showed no apparent damage.

Boney Courthouse

Boney Courthouse was built in 1970 in downtown Anchorage and retrofitted with CFRP in 2009 per ASCE/SEI 41 (2017). The target performance objective was between Life Safety and Immediate Occupancy. The CFRP was applied to walls in both directions, as well as a few beams. Some of the courthouse shear walls were retrofitted with six to seven plies of CFRP to achieve the desired load-carrying capacity increase. It was recognized by an engineer who worked on the project that the large number of CFRP plies became less economical at six to seven plies as the number of CFRP plies is inversely proportional to the effective strain in CFRP at debonding (ACI 440.2R). Applying more than two to three plies of CFRP also poses constructability problems as thicker fiber fabric can sag under

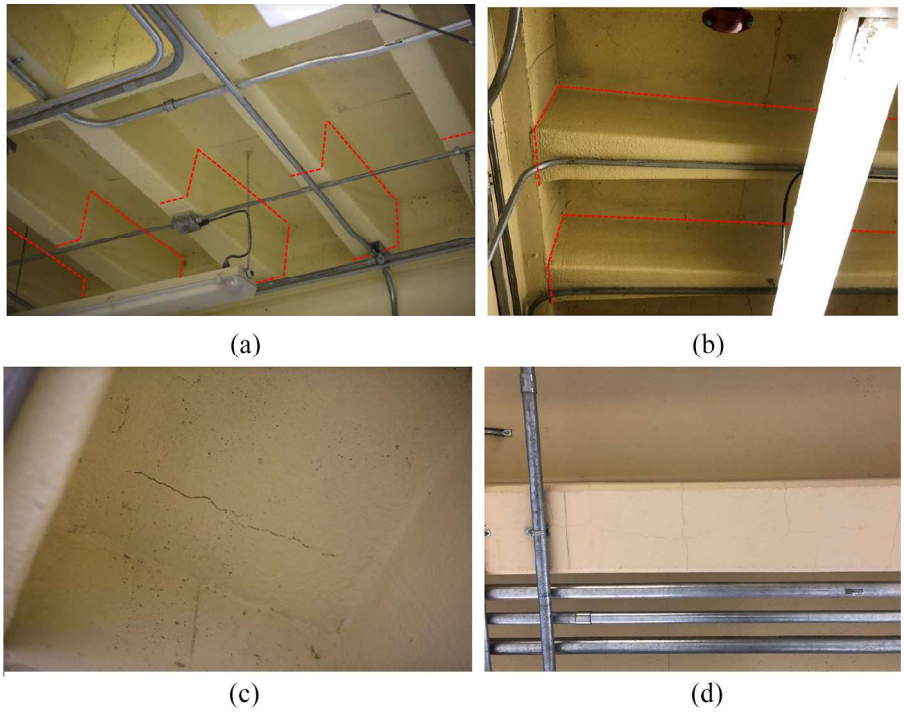

Figure 7. (a and b) Beams retrofitted with CFRP as denoted by dotted red lines, (c) cracking in the supported roof slab, and (d) minor cracking in a beam that was not FRP retrofitted.

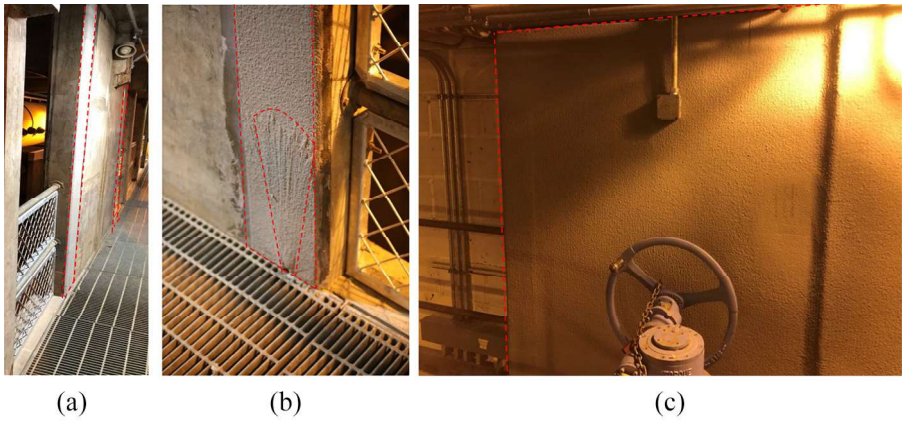

Figure 8. (a) Boundary element with CFRP denoted with a red dotted line, (b) boundary element with CFRP anchored with a splayed fiber anchor where CFRP and anchor perimeter are marked by red dashed line, and (c) a horizontally wrapped GFRP shear wall denoted with a red dotted line wrapped 30 cm behind this wall for confinement.

its self-weight and can generate significant heat due to the large thickness of the exothermically curing epoxy adhesive. The CFRP retrofit was primarily applied on one side of

the walls. Most of the CFRP-retrofitted shear walls in the courthouse were covered with paint, grout, drywall, or paneling. The one CFRP retrofit that the team was able to look at was accessed through the ceiling grid (Figure 9). No earthquake damage was observed on the side of the walls retrofitted with EBFRP. In multiple one-sided retrofitted walls, hairline cracks were observed on the non-retrofitted side, but it is not known whether or not those cracks existed before the earthquake. This observation illuminated the need for inspection tools that can assess the condition of the concrete underneath the CFRP.

Joint Base Elmendorf–Richardson

At Joint Base Elmendorf–Richardson (JBER), the Engineering Squadron building was inspected. Based on the visual inspection and information provided by building owners, location of the EBFRP-strengthened members was determined. A single interior beam was CFRP-retrofitted on one side to improve the shear transfer capacity between the beam and the masonry wall (Figure 10a). This CFRP retrofit was added when nearby interior shear walls were removed. Steel bracing was used throughout the rest of the building for seismic bracing. No damage was observed in the retrofits inside of the buildings. On the outside of the building, roughly half of the masonry walls were retrofitted with CFRP but were covered with stucco. These CFRP retrofits extended into the foundation for improving the shear transfer between walls and the foundation (Figure 10b). Some painted CFRP retrofit was exposed near the foundation and no apparent damage to it was observed. The backside of the CFRP-retrofitted walls on the interior of the building were in good condition with no apparent damage.

Figure 9. CFRP retrofit above ceiling grid covered by drywall panels at Boney Courthouse.

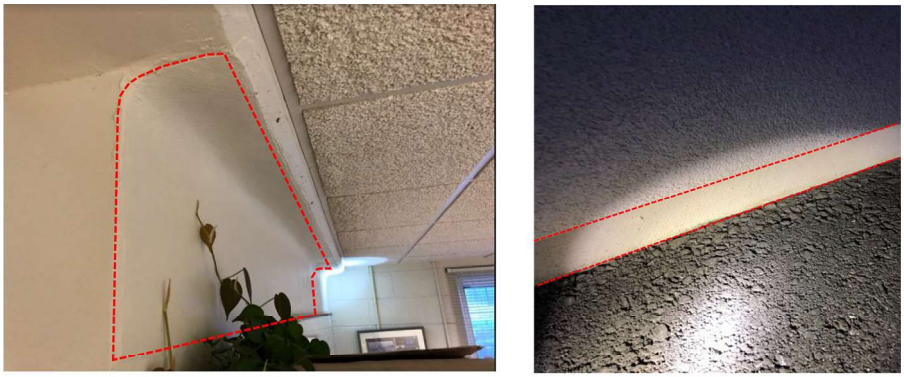

(a) (b)

Figure 10. CFRP application (a) to transfer shear between the reinforced concrete beam and the wall, and (b) to transfer shear between the outer wall and the foundation. CFRP retrofits are denoted by a red dotted line.

Ted Stevens International Airport

The TSIA underwent a significant retrofit in 2010. The retrofit involved addition of shear walls that were tied to existing columns. Consequently, the seismic demand on the columns was increased, thus necessitating strength and ductility improvements. Many columns were entirely or partially wrapped with two to three plies of CFRP to be able to sustain the imposed design demands. Our inspection included two interior and multiple exterior columns.

Visual inspection—interior column. An interior column of the checked-in baggage screening area of TSIA (South terminal) was retrofitted with two or three plies of CFRP for confinement. The column had a square cross-section measuring 40 cm $\times$ 40 cm. CFRP was coated with a beige paint. The overlap splices between different CFRP sheets were approximately 2.5 cm wide. The adjacent concrete columns were unwrapped as there was no additional axial load transferred to them. No obvious signs of earthquake damage were observed on retrofitted and non-retrofitted columns. The retrofitted column was inspected for debonding along one face using IR thermography and acoustic sounding (see section "CFRP debonding"). A second FRP-retrofitted (with two or three plies) interior column in the stairwell leading out to the tarmac was also inspected visually and with acoustic sounding. This second column was retrofitted for improved seismic performance and had no visible signs of damage or large debonded areas. This column was not inspected further since the accessible surface area of the retrofitted column was small.

Visual inspection—exterior columns. Three exterior columns retrofitted with CFRP, measuring 60 cm $\times$ 60 cm in cross-sectional dimension, on the south side of TSIA were also inspected (Figure 11). These three columns were entirely or partially wrapped with two to three plies of CFRP to be able to sustain the imposed design demands. Exterior column #1 was located adjacent to a wall, so the CFRP retrofit on three sides of the column was

Figure 11. Exterior columns (a) #1, (b) #2, and (c) #3 at TSIA.

exposed (Figure 11a). Overlap splices between CFRP wraps were approximately 2.5 cm. The column had a cement-like protective coating and demonstrated signs of impact damage from vehicles or luggage, owing to its location near a baggage handling area. No obvious signs of earthquake damage were observed. Exterior columns #2 and #3 were positioned between two walls, with only one face of their CFRP retrofits exposed. Debonded areas were identified by acoustic sounding on columns #2 and #3 and were marked with a blue painter's tape (Figure 11). Column #1 was also evaluated by IR thermography (see section "CFRP debonding"). Three bond pull-off tests were conducted on each column and discussed in the section "Bond pull-off test results."

CFRP debonding. IR thermography combined with acoustic sounding was used on the interior column and exterior column #1. Exterior columns #2 and #3 were evaluated for debonding by acoustic sounding only. The quantitative results for these four columns are summarized in Table 2. Data indicate that debonding was more severe for the exterior columns #1 and #2 than the interior column and exterior column #3 (Table 2). The debonded areas on the interior column were within the size range (between 1300 and 16,000 mm^2) that should be repaired by resin injection, per ACI 440.2R. Five out of eleven debonded areas on the exterior columns #1 and #2 exceeded the area of 16,000 mm^2 which, per ACI 440.2R, should be repaired by cutting out the affected sheet and applying and an overlapping CFRP patch at the top of it. Exterior column #3, by contrast, had a few debonded areas that were of relatively small size, similar to those observed on the interior column.

Since CFRP retrofits' purpose is to provide confinement to the columns, which falls under contact-critical applications, the debonding would generally not be a concern. However, it should be noted that recent evidence suggests that excessive debonding in contact-critical applications may reduce their effectiveness in providing confinement (Qin et al., 2019). It is worth mentioning that some current practices treat all the EBFRP applications as bond critical to prevent potential undesired failure modes and promote durability

Table 2. Summary of quantitative defect data at TSIA.

Property		Combined IR thermography and acoustic sounding		Acoustic sounding	
		Interior column	Exterior column #1	Exterior column #2	Exterior column #3
Total number of defects		13	5	6	4
Total area of defects (mm^2)		34,350	173,000	49,377	4335
Total area inspected (mm^2)		1,600,000	2,400,000	810,000	810,000
Defects of area inspected (%)		2	7	6	< 1
Defect area (d) classification per ACI 440.2R	$d < 1300$ mm^2	2	0	0	3
	1300 $mm^2 \leq d \leq$ 16,000 mm^2	11	1	5	1
	$d >$ 16,000 mm^2	0	4	1	0
Average defect area ± Standard deviation (mm^2)		2454 ± 1520	34,600 ± 33,680	8230 ± 8320	1084 ± 408
Maximum defect area (mm^2)		5800	94,000	24,545	1682
Minimum defect area (mm^2)		700	10,000	1658	815

TSIA: Ted Stevens International Airport; IR: infrared; ACI: American Concrete Institute.

(National Cooperative Highway Research Program (NCHRP), 2008). However, it is not clear to the authors whether the same approach was adopted to initially retrofit the columns at TSIA. Inspection reports following the original CFRP installation were not available, so the source and timeframe of debonding were not evident. The debonding could have resulted from installation defects, long-term environmental aging, the earthquake loading, or a combination thereof. It should be noted that the interior column had lower levels of debonding that could be due to inconsistencies in the installation process. Debonding data were corroborated against bond pull-off test results, discussed later in the article, and additional discussion of possible sources of debonding are provided.

Bond pull-off test results. Table 3 summarizes bond strengths and the corresponding failure modes from pull-off tests. Adhesion strength in 7 out of 12 pull-off experiments were below the ACI 440.2R minimum requirement of 1.4 MPa (200 lbf/in^2) and exhibited complete or partial Mode E, indicating flawed adhesion between CFRP and concrete (Table 3).

The interior column, which was not subjected to extreme environments, displayed relatively low bond strength values. However, besides test I-1, which exhibited low adhesive bond strength by failure Mode E due to a lack of surface preparation, the failure modes on this column were dominated by Mode G, indicating good adhesion between the CFRP and substrate. The low bond test strengths can, thus, be attributed to low substrate strength in I-2 and I-3. Close examination of the pulled-off substrate materials suggests the presence of cement paste and sand without any larger coarse aggregate grains leading the authors to believe that some type of mortar was used on the column surface prior to retrofit installation. This finding highlights the importance of ensuring a sound bonding substrate when the quality of the bond is considered during design.

Table 3. Bond pull-off test results for TSIA.

Location	Test #	Bond strength (MPa)	Failure mode	Failure mode on EBFRP
Interior column	I-1	1.03 (149 lbf/in^2)	Mode E[a]	
	I-2	Inconclusive	Mode F (~90% Mode G, ~10% Mode E[a])	
	I-3	1.23 (179 lbf/in^2)	Mode G	
Exterior column #1	E1-1	January 2019: 1.36 (198 lbf/in^2) Re-tested September 2019: 1.07 (155 lbf/in^2)	January 2019: Mode A[b] Re-tested September 2019: Mode F (~40% Mode G, ~60% Mode E[a])	
	E1-2	0.57 (82 lbf/in^2)	Mixed failure mode (~25% Mode E, ~75% Mode C[a])	
	E1-3	0.61 (88 lbf/in^2)	Mode F (~25% mode G, ~75% mode E[a])	

(continued)

Table 3. Continued

Location	Test #	Bond strength (MPa)	Failure mode	Failure mode on EBFRP
Exterior column #2	E2-1	3.43 (498 lbf/in^2)	Mode F (~20% Mode G, ~80% Mode E[a])	
	E2-2	0.72 (104 lbf/in^2)	Mode E[a]	
	E2-3	0.69 (100 lbf/in^2)	Mode F (~20% Mode G, ~80% Mode E[a])	
Exterior column #3	E3-1	>3.86[a]	No failure[c]	N/A
	E3-2	>3.19	Mode A[b]	N/A
	E3-3	>3.86[a]	No failure[c]	N/A

TSIA: Ted Stevens International Airport; N/A: not applicable; EBFRP: externally bonded fiber-reinforced polymer.
[a]Mode E likely varied visually due to non-uniform surface preparation, uneven application of paste epoxy (also known as putty), and/or entrapped air bubbles along the EBFRP–concrete interface. Mode E was identified based on the smooth surface and the lack of aggregate observed.
[b]Mode A indicates that reported adhesion strength values represent lower bound on EBFRP–concrete adhesion strength.
[c]Load limit of the adhesion tester was reached before failure occurred; thus, reported values represent the lower bound of EBFRP–concrete adhesion strength.

In the pull-off test experiments conducted on exterior columns #1 and #2, the failure surface was not flat, pointing to possible bond degradation or inconsistencies in initial surface preparation. The occurrence of Mode E and low bond pull-off strength values were in good correlation with the debonding observed with acoustic sounding and IR thermography on exterior columns, which implies that CFRP retrofits on exterior columns #1 and #2 were likely affected by environmental degradation or inconsistent surface preparation. It should also be noted that immediately following the pull-off experiments on exterior column #2, a damp concrete surface was noted underneath the retrofit, which indicated that moisture was accumulating in the underlying concrete substrate (this was not observed on exterior column #1 in January during low temperature conditions). The observed dampness further suggests that environmental effects from freeze–thaw may have contributed to the low pull-off strength, if not being completely responsible for poor adhesion between CFRP and concrete on this column. Interestingly, exterior column #3 was an anomaly as all three bond pull-off strength values on exterior column #3 exceeded the load capacity of the adhesion tester and passed the minimum ACI bond strength requirements. Although columns #2 and #3 similarly had one face on the interior and the other one on the exterior of the building, the different pull-off test strengths could be due to possible differences in

moisture transport from the interior of the concrete to the exterior EBFRP/concrete interface at different locations in the building. Moisture transport from the interior of the concrete could occur from temperature gradients that form between the interior and exterior of the concrete (depending on the level of concrete insulation), which could lead to condensation below the dew point and subsequent moisture transport to the EBFRP/concrete bond. Capillary transport of moisture from the soils below the concrete to the EBFRP/concrete bond may also have occurred. In both cases, moisture build-up at the EBFRP/concrete interface can lead to expansion and internal stress at the interface during freeze–thaw. While the source of moisture in column #2 cannot be definitively determined based on the available information, it is possible that moisture transport from the building interior at exterior column #2 location was more severe than in exterior column #3, leading to accelerated CFRP–concrete bond deterioration. Furthermore, exterior column #2 and exterior column #1 both had signs and non-structural components attached with bolts that went through the CFRP and may have led to exterior water ingress that would not be present in exterior column #3. Inconsistent surface preparation may have created voids at the EBFRP/concrete interface, which became locations where moisture transport from the concrete occurred. Cracks or debonded areas at the EBFRP/concrete interface, formed from differences in thermal expansion of concrete and CFRP at low temperatures, may have also provided additional sites of moisture transport from the concrete. In both scenarios, freeze–thaw expansion stresses of moisture may have contributed to the low pull-off strengths and Mode E failures on exterior columns #1 and #2.

Although installation procedures, location, and environmental conditions were similar for exterior column #3 and exterior columns #1 and #2, bond pull-off test results were in significant disagreement, which poses concerns regarding the ability of the ASTM D7522 test method to adequately assess quality of bond by sampling locations selected at random. This issue could potentially lead to different retrofit or repair decisions depending on the selected structural component and the location of the pull-off test on the retrofitted component. Further guidance on the number of pull-off tests and locations of the test, especially since the pull-off test is so localized, are needed for clearer assessment of bond strength and failure mode. Although columns are contact critical, the failure modes were often not Mode G in bonded areas and pull-off tests are the only real means of assessing bond strength and bond failure modes. Thus, records of initial pull-off tests should be maintained as a baseline for comparison to pull-off tests conducted during inspection of EBFRP retrofits used in service over the long term to adequately assess durability concerns for both contact-critical and bond-critical applications.

MKT

MKT was the first building retrofitted with EBFRP in Anchorage. The 14-story structure experienced significant damage in the 1964 Great Alaskan Earthquake (M_w 9.2) involving cracking in exterior walls, shear failure of the spandrel beams, and cracking along construction joints (Ehsani, 2007). In 1998, a seismic retrofit was started involving the addition of shear walls, enlargement of existing columns, the addition of structural steel members, and upgrades of the structure's foundation system. Due to the excessive cost of the traditional retrofit construction, the initial retrofit plan was completed only up to the fourth story. Then, EBFRP retrofits were selected to complete the work, given their significantly lower cost. EBFRP retrofits that were installed in 2004 were used for shear wall strengthening, column confinement, shear strengthening of coupling beams, and flexural strengthening of the roof slab. CFRP was used specifically for shear wall strengthening, flexural and

shear strengthening of cantilever beams, and flexural strengthening of a roof slab. GFRP was used specifically for column confinement, shear wall strengthening, and boundary element strengthening. Additional details about the EBFRP retrofits can be found elsewhere (Ehsani, 2007). It was unclear whether any exterior EBFRP retrofits were considered strictly contact critical and in many cases were likely bond critical.

Visual inspection. No apparent earthquake damage to the EBFRP retrofits was observed in the post-earthquake inspections (Figure 12). However, like other inspected structures, most of the retrofitted structural components were not directly accessible as they were covered with nonstructural elements or architectural features. A few interior columns were identified as having exposed GFRP. Exterior GFRP and poorly epoxy-saturated carbon fibers on the North and South side of MKT, which manifested itself with readily apparent exposed dry fibers; fully saturating EBFRP with epoxy during wet layup in the field is known to be a common challenge and can possibly contribute to debonding (Figure 13a and b). Premature debonding is one of the main drawbacks of EBFRP-retrofitted systems and significant research effort has been made to develop effective anchoring using EBFRP spike anchors. Similar to EBFRP sheets installations, installation of EBFRP anchors depends on the skill of the installer and is critical for adequate performance (del Rey Castillo and Kanitkar, 2020; Grelle and Sneed, 2013). The authors also reported that inadequate fiber saturation can significantly affect the effectiveness of EBFRP-strengthened system. Exposed retrofits at MKT were evaluated for debonding by acoustic sounding. Quality of bond between EBFRP and concrete was assessed by bond pull-off tests.

EBFRP debonding. Exposed GFRP and CFRP were evaluated for debonding by acoustic sounding. Besides minor localized defects, no debonding was observed in the GFRP retrofits, both on the interior and exterior of the structure. Exterior CFRP retrofits, however, exhibited areas of debonding as shown in Figure 14. Similar to some CFRP retrofits at TSIA, moisture was observed below the exterior CFRP retrofits at MKT in some cases and might have contributed to the debonding observed (Figure 13c and d).

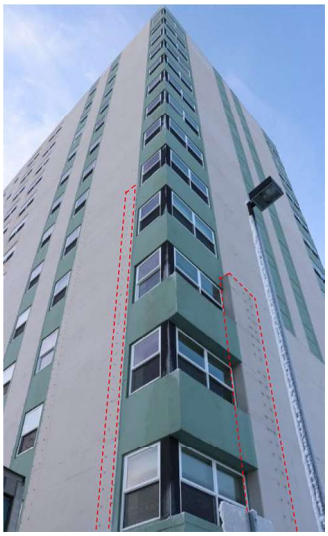

Figure 12. Boundary elements confined with EBFRP and bolts on MKT, marked by red dashed lines.

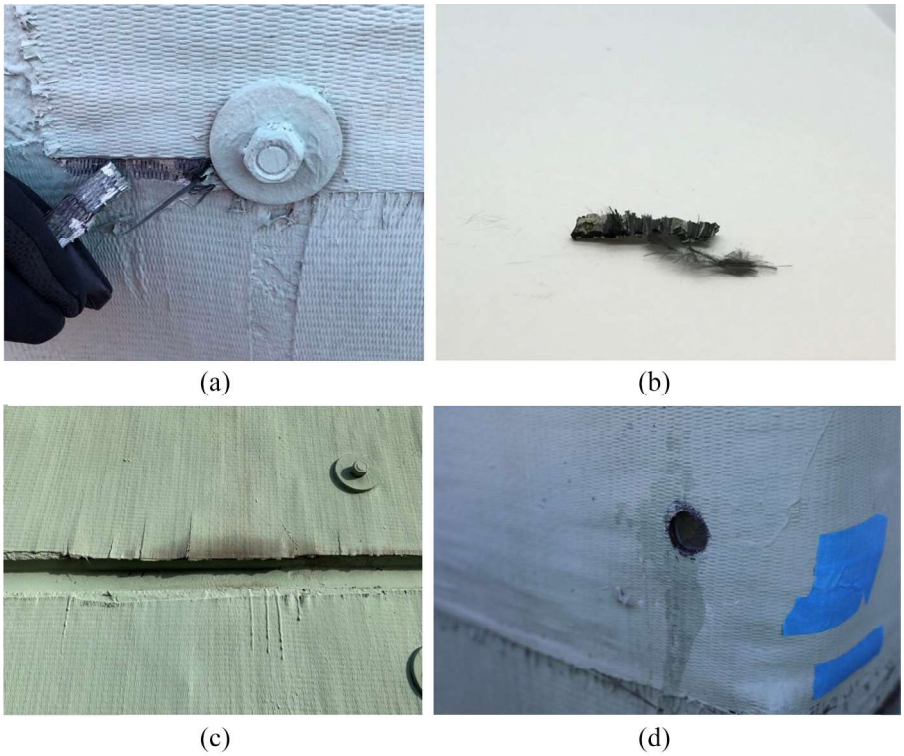

Figure 13. Exterior CFRP debonding (marked by blue painter's tape) on a boundary element at MKT: (a) front view and (b) side view from the window well.

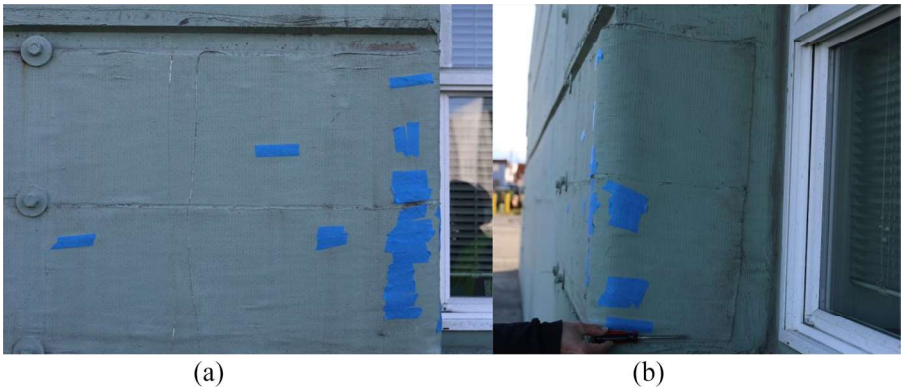

Figure 14. Exterior CFRP retrofits at MKT: (a) One area and (b) a collected CFRP sample from CFRP locations with poor epoxy saturation and (c and d) areas where moisture or water was present.

Bond pull-off test results. Bond pull-off tests were conducted on an interior column located in a closet of an apartment on the sixth floor of MKT, and along the exterior south side wall (CFRP) and east shear wall (GFRP). Bond strength data and the accompanying failure modes are summarized in Table 4.

Table 4. Bond pull-off test results for McKinley Tower.

Location	Test #	Bond strength (MPa)	Failure mode	Failure mode on EBFRP
Interior column (GFRP)	I-1	3.50 (508 lbf/in^2)	Mode F (~80% Mode G, ~20% Mode E[a])	
	I-2	2.65 (384 lbf/in^2)	Mode G	
Exterior location #1 (GFRP)	E1-1	$>$ 3.86 ($>$ 560 lbf/in^2)	No failure[b]	N/A
	E1-2	$>$ 2.13 (309 lbf/in^2)	Mode A	N/A
Exterior location #2 (GFRP)	E2-1	$>$ 3.86 ($>$ 560 lbf/in^2)	Mode G	
	E2-2	1.37 (199 lbf/in^2)	~30% Mode A, ~65% Mode E, ~5% Mode G	
Exterior location #3 (CFRP)	E3-1	0.74 (107 lbf/in^2)	Mode E[a]	
	E3-2	1.25 (182 lbf/in^2)	Mode E[a]	
	E3-3	1.21 (176 lbf/in^2)	Mode E[a]	

GFRP: glass fiber–reinforced polymer; N/A: not applicable; EBFRP: externally bonded fiber-reinforced polymer.
[a]Mode E likely varied visually due to non-uniform surface preparation, uneven application of paste epoxy (also known as putty), and/or entrapped air bubbles along EBFRP–concrete interface. Mode E was identified based on the smooth surface and the lack of aggregate observed.
[b]Load limit of the adhesion tester was reached before failure occurred.

Pull-off tests on GFRP exceeded the minimum ACI 440.2R bond strength requirement, with the exception of test E2-2, which was only slightly below 1.4 MPa (200 lbf/in^2). Mode G was the most dominant failure mode in GFRP, except for the exterior E2-2 test that failed by Mode E. The failure surface of the E2-2 test location was smooth and appeared to contain some paint, indicating a lack of surface preparation, which explains the relatively low pull-off bond strength value. Overall, there was little difference among interior and exterior pull-off test results, which suggested that exposure to the outdoor environment did not adversely affect the bond of GFRP to concrete.

All three pull-off tests on CFRP did not meet the minimum pull-off bond strength requirement of 1.4 MPa (200 lbf/in^2). Each of the tests resulted in Mode E failure, indicating poor adhesion between epoxy and concrete. In contrast to the condition of the exterior GFRP retrofits at MKT, the exterior CFRP retrofits at MKT and TSIA had more debonding, lower pull-off bond test strength, and greater occurrence of Mode E failure. One possible explanation for comparatively lower bond performance of CFRP retrofits when compared to GFRP is the difference in CTEs and elastic modulus between the two materials (Table 5). From this comparison, under the wide temperature swings characteristic of Anchorage, AK, the mismatch in thermally induced bond stresses would be much greater between concrete and CFRP than between concrete and GFRP. For CFRP specifically, the CTE is typically negative and leads to expansion under temperatures close to and below freezing while concrete has a positive CTE and contracts under the same conditions. Even though care is often taken to maintain CTE of CFRP close to zero by proper composite design and selection of adequate epoxy matrix, the thermally induced stresses at CFRP–concrete interfaces would be orders of magnitude greater than those in GFRP–concrete interfaces due to the relatively high mismatch in CTE and elastic modulus between CFRP and concrete. Moisture transport in combination with freeze/thaw was also likely an issue at MKT, as moist concrete or water was observed under some of the CFRP retrofits after pull-off tests. Moisture transport was observed for CFRP retrofits but not GFRP retrofits, possibly due to differences in exterior water entry at the CFRP and GFRP testing locations used, localized differences in initial installation quality, which led to moisture uptake in voids present at the CFRP/concrete interface, or CFRP debonding or cracks formed from CTE mismatch that allowed for moisture uptake from the concrete.

Table 5. Thermal and elastic properties of normal strength concrete, GFRP, and CFRP.

Property	Normal-strength concrete	GFRP	CFRP
Coefficient of thermal expansion (longitudinal)	7 to 11 $\times$ 10^{-6}/°C[a]	6 to 10 $\times$ 10^{-6}/°C[b]	–9 to 0 $\times$ 10^{-6}/°C[b]
Elastic modulus	20–30 GPa[c]	23–72 GPa[d]	96–300 GPa[d]

[a]Mindess et al. (2003).
[b]ACI 440.1R-15 (2015).
[c]ACI 318-19 (2019).
[d]ACI 440R-07 (2007).

Discussion of observations in reference to existing literature

Earthquake effects cannot be decoupled from environmental aging and both can result in similar types of damage, most notably, debonding. Field studies are valuable for future retrofit design, but without information on pre-earthquake condition, post-earthquake damage assessment is difficult. Since baseline data on EBFRP retrofits at TSIA and MKT were not available, discussion was limited to presenting potential reasons for some of the observed low bond strengths and debonding. As an addition to the discussion of results of field inspection observations, comparison with durability studies by other researchers in cold aseismic regions is presented. Observations of earthquake damage at different loading levels in EBFRP-retrofitted RC structures as reported in the literature are also provided.

The range of pull-off bond strength values measured at TSIA (82 to 560 lbf/in^2) and MKT (107 to 560 lbf/in^2) seems to be consistent with values reported by other researchers. Pull-off bond strength measured on four bridges strengthened with CFRP and GFRP in Canada varied between 0.83 MPa (120 lbf/in^2) and 3.54 MPa (513 lbf/in^2; Banthia et al., 2010). Failures occurred in the repair mortar, concrete substrate, or at the EBFRP/concrete interface. Higher bond strengths were measured on GFRP than CFRP repairs. Tests conducted on a bridge in Colorado, 8 years after CFRP installation, showed that 9 of 27 tests had pull-off bond strength lower than 200 lbf/in^2 (Atadero and Allen, 2013). Specifically, the maximum measured pull-off bond strength on this bridge was 550 lbf/in^2. Over time, more failure modes at the EBFRP/concrete interface and more debonded areas were observed than at the time of bridge repair. This was accompanied by a decrease in mean bond strength from 2.98 MPa (432 lbf/in^2), measured initially at CFRP installation, to 1.93 MPa (279 lbf/in^2). As an exception, in a study by Siavashi et al. (2019), higher bond strengths were measured on free-standing columns after 15 years of service in Michigan—values varied between 215 and 1032 lbf/in^2, with an average of approximately 600 lbf/in^2. Due to missing data on the original bond strength, specimens were recreated in the laboratory using the same materials that were used for the bridge repairs. Comparison of pull-off bond strength measured after 15 years of long exposure with the initial strength (which was also relatively high compared to values reported in Atadero and Allen (2013) measured on the recreated specimens, showed that considerable degradation of strength (approximately 30%) occurred. Similar to the two studies referenced above (Atadero and Allen, 2013; Banthia et al., 2010), change in failure modes from Mode G to Mode F and Mode E, was observed here too. Insufficient saturation of CFRP fabric and the presence of air bubbles at the failure surface were indicated as reasons for failure of the EBFRP and adhesive. Range of measured bond strength (Atadero and Allen, 2013; Banthia et al., 2010) and observations related to CFRP performance with respect to GFRP are similar to the results of bond evaluation at TSIA and MKT. The occurrence of adhesive failure modes in aged structures is also consistent with our observations. This suggests that factors such as surface preparation, quality of installation, and moisture in combination with freeze–thaw cycles had the most significant effect on bond strength. Effects of weathering on the bond, as a critical parameter for an efficient EBFRP system, should be considered in future design guidelines, since current guidelines consider environmental effects on the mechanical properties of the composite only.

To the best of authors' knowledge, there are no published data on the effect of earthquake loading on EBFRP/concrete bond strength. Existing studies of seismic performance of EBFRP-retrofitted structures are mostly focused on the structural behavior near

collapse. There is a limited understanding of how shaking events of lower intensity than a design-level earthquake affect EBFRP retrofit performance. Shin et al. (2016) evaluated damage in a full-scale CFRP-retrofitted RC frame at different loading levels. Specifically, natural frequency, inter-story drift and column and beam rotations were measured. Effectiveness of CFRP retrofits was evaluated by comparing test results with (1) damage limits based on FEMA interstory drift and hinge rotations prescribed in ASCE 41-13 and (2) corresponding tests results obtained on the unretrofitted frame. During initial loading stage (for drift ratio lower than 1%) no visible damage was observed in the structure or CFRP; however, a decrease in natural frequency of the frame was reported, which indicates that some damage was occurring. The importance of residual performance of EBFRP-retrofitted columns after limited seismic damage has already been recognized (Shan et al., 2006), however, research data on this issue are scarce. Realfonzo and Napoli (2009) showed that stiffness degradation and associated increasing drift is independent of the EBFRP confinement. Further research on residual performance of contact-critical applications focusing on the mechanism of stiffness reduction after limited damage of EBFRP-strengthened system would be valuable for damage mitigation in subsequent earthquakes.

From the previous discussion, it is clear that post-earthquake damage detection by visual inspection in EBFRP RC structures is quite limited, especially when they are exposed to lower intensity earthquakes, since EBFRP conceals concrete cracks, voids, and debonding. In some cases, signs of CFRP damage are not visible even at a drift ratio of 9% (Ma et al., 2000). Quasi-static testing of CFRP-strengthened shear walls showed that at ultimate load, failure initiates by compressed concrete crushing, which is followed by fracture of tension reinforcing bars and finally rupture of EBFRP sheets at the base of the wall (Lombard et al., 2000). Having in mind that visible damage of EBFRP (e.g., rupture of EBFRP) typically occurs in the final loading stage, evaluation of damage due to earthquakes with intensities lower than design earthquake requires more sophisticated methods. Non-destructive evaluation (NDE) methods, typically used by inspection engineers, have the disadvantage of requiring contact with the tested structure. Even if better NDE methods were used for field inspection, lack of baseline data is another issue that makes damage assessment challenging. For example, debonding observed at exterior column #1 at TSIA cannot be attributed with certainty to the earthquake, environmental degradation, or installation defects. It is reasonable to include earthquake effects as one of the potential reasons for observed debonding, having in mind that EBFRP debonding can occur in walls at very low drift ratios from 0.16% to 0.46% (Cruz-Noguez et al., 2015). The inability to confirm the exact cause(s) of debonding observed at TSIA due to the lack of baseline data warrants further field studies where appropriate controls are established.

Summary and conclusion

Following the 2018, magnitude 7.1, Cook Inlet earthquake in Anchorage, AK, a reconnaissance team consisting of researchers from the University of Delaware Center for Composite Materials and the NIST visited Anchorage, AK, to assess the performance of EBFRP retrofits following the earthquake as well as the condition of EBFRP after extended ($>$ 10 years) exposure to a harsh subarctic climate. The work was conducted over two visits, in January and September 2019. The scope of inspections included seven retrofitted structures and consisted of (1) visual inspection to identify visible signs of

earthquake damage to EBFRP retrofits, (2) acoustic sounding and IR thermography to identify debonded areas, and (3) bond pull-off tests to evaluate bond quality in EBFRP retrofits. This study looked at both the seismic performance of EBFRP-retrofitted structures following the Cook Inlet Earthquake and the condition of the EBFRP retrofits after long-term outdoor exposure, which can have an impact on EBFRP retrofit performance. The following conclusions were made based on the presented work:

1. No apparent signs of earthquake damage to EBFRP retrofits were observed. This could be partially because the 2018 ground motion spectral acceleration did not exceed the design-level earthquake for most structures in Anchorage, AK. Further study on EBFRP-retrofitted structures following other significant shaking events will be warranted.
2. IR thermography, acoustic sounding, and pull-off strength data indicate that some bond degradation may have occurred in exterior CFRP retrofits.
3. Observed debonding cannot be attributed with certainty to the earthquake, environmental degradation, or installation defects due to the lack of pre-earthquake condition assessment data.
4. Comparison of debonding and bond pull-off strength data between GFRP and CFRP suggests that the CFRP–concrete bond is more vulnerable to deterioration under a subarctic climate than a GFRP–concrete bond. It is hypothesized that this is due to the greater mismatch in CTE and elastic modulus between concrete and CFRP than concrete and GFRP. Other field variables, such as the effectiveness of concrete surface preparation, installation procedure, and transport of moisture from the concrete to the EBFRP/concrete interface or exterior ingress of moisture, could have contributed to the observed difference in bond durability between GFRP and CFRP under expansive stresses related to freeze–thaw cycles.

Recommendations

Based on the work presented here, the following practical recommendations and topics requiring further research were identified:

- Pull-off test results on the TSIA interior column were determined to be relatively low (i.e. below ACI 440.2R requirement) due to a lack of surface preparation at one test location and low substrate strength. It is suggested that substrate and any repair materials used to level the surface prior to EBFRP installation be tested via pull-off bond test to ensure the substrate meets a minimum pull-off strength of 1.4 MPa. This is deemed especially important in exterior EBFRP applications where surface layers of the substrate might be deteriorated and exhibit reduced pull-off strength, even though compression tests on field-extracted concrete core samples may indicate otherwise. When bond between EBFRP and concrete is sound and free of defects, the lower bound on the bond strength is limited by the tensile strength of the concrete surface (rather than the bulk of the material).
- The pull-off test provides localized information about the quality of bond between EBFRP and concrete substrate. Depending on the structural components selected for the test, the location of the tests, and the number of tests, different conclusions can be made on the bond quality, which in turn can lead to different retrofit/repair

decisions. This issue warrants a more global method for assessing the EBFRP–concrete bond quality in practice as well as more clear guidelines on the location and number of pull-off tests. Furthermore, because there is no guidance on evaluating bond strength and failure mode in contact-critical applications (i.e. on columns), pull-off tests still need to be employed to assess changes due to environmental aging. Baseline pull-off test data need to be collected and recorded immediately following initial EBFRP installation for comparison to pull-off tests conducted on EBFRP retrofits in service for long periods of time.

- Establishing baseline data for pull-off tests and composite mechanical properties at the time of installation or immediately thereafter were not possible in this study due to the lack of documentation of quality control data. It is suggested that in future projects, EBFRP witness panel tensile test data, bond pull-off test data, and any other information collected pre-, during, and post-construction be well-documented and preserved. In the future, accessibility to these data might allow engineers to establish effectiveness of the retrofits following extreme loadings.
- IR thermography can be used to identify defects in EBFRP retrofits, but it should be used in conjunction with acoustic sounding to remove any "false positive" readings. The data collection process is time-consuming and offers minimal benefits over simple acoustic sounding. Methods should be developed that will allow automated defect recognition from IR thermographs.
- Most EBFRP retrofits are covered with non-structural panels making it difficult to assess the condition of EBFRP. This is problematic because it could lead to reliance on potentially ineffective retrofits. Future research should develop and implement self-sensing methods and non-destructive techniques that will allow to properly assess the condition of EBFRP covered by non-structural components following extreme events (such as earthquakes). In addition, access panels to EBFRP retrofits would help inspectors following seismic events and for long-term inspection of durability.
- The effects of climate are rarely explicitly considered in material selection for EBFRP retrofit design. While CFRP is generally thought to be more durable than GFRP (ACI 440.2R), our field data suggest that GFRP, particularly with respect to bond durability, might be more appropriate for subarctic environments than CFRP. Additional research should be performed to better characterize the behavior of GFRP and CFRP bond to concrete under freeze–thaw cycles, develop predictive analytical models to evaluate environmentally induced bond stresses, and ultimately, develop performance-based design guidelines that consider climate effects with respect to EBFRP materials selection. Future studies should investigate how degraded state of EBFRP-retrofitted structures affects their performance during earthquake. The effect of initial bond quality and moisture are also necessary considerations during freeze–thaw cycle testing.

NIST Disclaimer: Certain commercial products or equipment are described in this article to adequately specify the experimental procedure. In no case does such identification imply recommendation or endorsement by the NIST, nor does it imply that it is necessarily the best available for the purpose.

Acknowledgments

The authors would like to thank Quakewrap Inc. and Jeff Robertson, PE from Quakewrap Inc. for their assistance before and during this reconnaissance effort. The authors also gratefully acknowledge the building/site owners and managers who provided access and permission to inspect EBFRP retrofits.

Declaration of conflicting interests

The author(s) declared no potential conflicts of interest with respect to the research, authorship, and/or publication of this article.

Funding

The author(s) disclosed receipt of the following financial support for the research, authorship, and/or publication of this article: Tatar gratefully acknowledges financial support provided by the National Science Foundation (NSF) to the University of Delaware under award number 1916972. Any opinions, findings, and conclusions, or recommendations expressed in this article are those of the authors and do not necessarily reflect the views of the NSF or National Institute of Standards and Technology.

ORCID iDs

Jovan Tatar https://orcid.org/0000-0003-4901-4019
David Goodwin https://orcid.org/0000-0002-5979-3581

References

ACI 318-19 (2019) Building code requirements for structural concrete and commentary.
ACI 440.1R-15 (2015) Guide for the design and construction of structural concrete reinforced with fiber-reinforced polymer bars.
ACI 440.2R (2017) Guide for the design and construction of externally bonded EBFRP systems for strengthening concrete structures.
ACI 440R-07 (2007) Report on fiber-reinforced polymer (FRP) reinforcement for concrete structures.
Al Azzawi M, Hopkins P, Mullins G and Sen R (2018) FRP-concrete bond after 12-year exposure in tidal waters. *Journal of Composites for Construction* 22(5): 1–15.
Al-Mahmoud F, Mechling JM and Shaban M (2014) Bond strength of different strengthening systems—Concrete elements under freeze-thaw cycles and salt water immersion exposure. *Construction and Building Materials* 70: 399–409.
ASCE/SEI 41 (2017) Seismic evaluation and retrofit of existing buildings (41-17).
ASTM D7522 (2015) Standard test method for pull-off strength for EBFRP laminate systems bonded to concrete substrate.
Atadero RA and Allen DG (2013) *Long term monitoring of mechanical properties of EBFRP repair materials*. Report No. CDOT-2013-13. Denver, CO: Colorado Department of Transportation.
Banthia N, Abdolrahimzadeh A, Demers M, Mufti A and Sheikh S (2010) Durability of FRP-concrete bond in FRP-strengthened bridges. *Concrete International* 32(8): 45–51.
Blackburn BP, Tatar J, Douglas EP and Hamilton HR (2015) Effects of hygrothermal conditioning on epoxy adhesives used in EBFRP composites. *Construction and Building Materials* 96: 679–689.
Bousias S, Spathis AL and Fardis MN (2007) Seismic retrofitting of columns with lap spliced smooth bars through EBFRP or concrete jackets. *Journal of Earthquake Engineering* 11(5): 653–674.
Brown JR (2005) *Infrared thermography inspection of fiber-reinforced polymer composites bonded to concrete*. PhD Dissertation, University of Florida, Gainesville, FL.
Cruz-Noguez CA, Lau DT, Sherwood EG, Hiotakis S, Lombard J, Foo S and Cheung M (2015) Seismic behavior of RC shear walls strengthened for in-plane bending using externally bonded EBFRP sheets. *Journal of Composites for Construction* 19(1): 04014023.
del Rey Castillo E and Kanitkar R (2020) Effect of EBFRP spike anchor installation quality and concrete repair on the seismic behavior of FRP-strengthened RC columns. *Journal of Composites for Construction* 25(1): 04020085.
del Rey Castillo E, Griffith M and Ingham J (2018) Seismic behavior of RC columns flexurally strengthened with EBFRP sheets and EBFRP anchors. *Composite Structures* 203: 382–395.

Di Ludovico M, Prota A, Manfredi G and Cosenza E (2008) Seismic strengthening of an under-designed RC structure with FRP. *Earthquake Engineering and Structural Dynamics* 37: 141–162.

Ehsani M (2007) Fiber reinforced polymers: Seismic retrofit of the McKinley Tower. *Structure Magazine*, July, pp. 35–37.

Goodwin DG, Sattar S, Dukes JD, Kim JH, Sung LP and Ferraris CC (2019) *Research needs concerning the performance of fiber reinforced (FR) composites retrofit systems for buildings and infrastructure*. Special Publication (NIST SP) - 1244. Gaithersburg, MD: National Institute of Standards and Technology.

Green MF, Bisby LA, Fam AZ and Kodur VK (2006) FRP confined concrete columns: Behaviour under extreme conditions. *Cement and Concrete Composites* 28(10): 028–937.

Green MF, Bisby LA, Beaudoin Y and Labossière P (2000) Effect of freeze-thaw cycles on the bond durability between fibre reinforced polymer plate reinforcement and concrete. *Canadian Journal of Civil Engineering* 27(5): 949–959.

Grelle SV and Sneed LH (2013) Review of anchorage systems for externally bonded EBFRP laminates. *International Journal of Concrete Structures and Materials* 7(1): 17–33.

Hag-Elsafi O, Alampalli S and Kunin J (2004) In-service evaluation of a reinforced concrete T-beam bridge EBFRP strengthening system. *Composite Structures* 64(2): 179–188.

Hamilton HR, Brown J, Tatar J, Lisek M and Brenkus NR (2017) *Durability evaluation of Florida's fiber-reinforced polymer (FRP) composite reinforcement for concrete structures*. Final Report for FDOT Contract No. BVD31-977-01. Gainesville, FL: University of Florida.

Kam WY, Pampanin S, Dhakal R, Gavin HP and Roeder C (2010) Seismic performance of reinforced concrete buildings in the 4th September 2010 Darfield (Canterbury) earthquake. *Bulletin of the New Zealand Society for Earthquake Engineering* 43(4): 340–350.

Kobatake Y (1998) A seismic retrofitting method for existing reinforced concrete structures using CFRP. *Advanced Composite Materials* 7(1): 1–22.

Lombard J, Lau D and Humar J (2000) Seismic strengthening and repair of reinforced concrete shear walls. In: *Proceedings of the 12th World Conference on earthquake Engineering*, Auckland, New Zealand, 30 January–4 February.

Ma CK, Apandi NM, Yung SCS, Hau NJ, Haur L, Awang AZ and Omar W (2017) Repair and rehabilitation of concrete structures using confinement: A review. *Construction and Building Materials* 133: 502–515.

Ma R, Xiao Y and Li KN (2000) Full-scale testing of a parking structure column retrofitted with carbon fiber reinforced composites. *Construction and Building Materials* 14(2): 63–71.

Mindess S, Young JF and Darwin D (2003) *Concrete*. 2nd ed. Upper Saddle River, NJ: Prentice-Hall.

Myers JJ and Sawant AV (2008) *Preservation of Missouri transportation infrastructures: Validation of EBFRP composite technology—Volume 5*. Report for MoDOT No. RI02-022. Rolla, MO: Missouri University of Science and Technology.

National Cooperative Highway Research Program (NCHRP) (2008) *Recommended construction specifications and process control manual for repair and retrofit of concrete structures using bonded EBFRP composites*. National Cooperative Highway Research Program (NCHRP), Report 609. Washington, DC: Transportation Research Board.

Pallempati H, Beneberu E, Yazdani N and Patel S (2016) Condition assessment of fiber-reinforced polymer strengthening of concrete bridge components. *Journal of Performance of Constructed Facilities* 30(6): 1–9.

Pan Y, Xian G and Li H (2018) Effects of freeze-thaw cycles on the behavior of the bond between CFRP plates and concrete substrates. *Journal of Composites for Construction* 22(3): 1–14.

Pantelides CP, Okahashi Y and Reaveley LD (2008) Seismic rehabilitation of reinforced concrete frame interior beam-column joints with EBFRP composites. *Journal of Composites for Construction* 12(4): 435–445.

Pendhari SS, Kant T and Desai YM (2008) Application of polymer composites in civil construction: A general review. *Composite Structures* 84(2): 114–124.

Qin R, Lau D, Tam L, Liu T, Zou D and Zhou A (2019) Experimental investigation on interfacial defect criticality of FRP-confined concrete columns. *Sensors* 19(3): 468.

Realfonzo R and Napoli A (2009) Cyclic behavior of RC columns strengthened by EBFRP and steel devices. *Journal of Structural Engineering* 135(10): 1164–1176.

Reay JT and Pantelides CP (2006) Long-term durability of state street bridge on Interstate 80. *Journal of Bridge Engineering* 11(2): 205–216.

Shan B, Xiao Y and Guo Y (2006) Residual performance of FRP-retrofitted RC columns after being subjected to cyclic loading damage. *Journal of Composites for Construction* 10(4): 304–312.

Sheikh SA and Tam S (2007) *Effect of freeze-thaw climatic conditions on long-term durability of EBFRP strengthening systems*. Final Report for Ministry of Transportation of Ontario, HIIFP-037. Toronto, ON, Canada: University of Toronto.

Shin J, Scott DW, Stewart LK, Yang CS, Wright TR and DesRoches R (2016) Dynamic response of a full-scale reinforced concrete building frame retrofitted with EBFRP column jackets. *Engineering Structures* 125: 244–253.

Siavashi S, Eamon CD, Makkawy AA and Wu HC (2019) Long-term durability of EBFRP bond in the Midwest United States for externally strengthened bridge components. *Journal of Composites for Construction* 23(2): 05019001.

Silva PF, Ereckson NJ and Chen GD (2007) Seismic retrofit of bridge joints in Central U.S. with carbon fiber-reinforced polymer composites. *ACI Structural Journal* 104(2): 207–217.

Tatar J and Hamilton HR (2016a) Comparison of laboratory and field environmental conditioning on FRP-concrete bond durability. *Construction and Building Materials* 122: 525–536.

Tatar J and Hamilton HR (2016b) Bond durability factor for externally bonded CFRP systems in concrete structures. *Journal of Composites for Construction* 20(1): 04015027.

Tatar J and Hamilton HR (2016c) Implementation of bond durability in the design of flexural members with externally bonded FRP. *Journal of Composites for Construction* 20(3): 04015072.

Tatar J, Brenkus NR, Subhash G, Taylor CR and Hamilton HR (2018a) Characterization of adhesive interphase between epoxy and cement paste via Raman spectroscopy and mercury intrusion porosimetry. *Cement and Concrete Composites* 88: 187–199.

Tatar J, Taylor CR and Hamilton HR (2019) A multiscale micromechanical model of adhesive interphase between cement paste and epoxy supported by nanomechanical evidence. *Composites Part B: Engineering* 172: 679–689.

Tatar J, Torrence CE, Mecholsky JJ Jr, Taylor CR and Hamilton HR (2018b) Effects of silane surface functionalization on interfacial fracture energy and durability of adhesive bond between cement paste and epoxy. *International Journal of Adhesion and Adhesives* 84: 132–142.

Tatar J and Milev S (2021). Durability of externally bonded fiber-reinforced polymer composites in concrete structures: A critical review. Polymers, 13(5), 765.

Triantafillou TC (1998) Shear strengthening of reinforced concrete beams using epoxy-bonded EBFRP composites. *ACI Structural Journal* 95(2): 107–115.

Woods JE, Lau DT and Erochko J (2020) Evaluation by hybrid simulation of earthquake-damaged RC walls repaired for in-plane bending with single-sided CFRP sheets. *Journal of Composites for Construction* 24(6): 04020073.